# Enhanced Electrical Conductivities of Complex Hydrides Li_2(BH_4)(NH_2) and Li_4(BH_4)(NH_2)_3 by Melting

Zhou, Yu
Institute for Materials Research, Tohoku University

Matsuo, Motoaki
Institute for Materials Research, Tohoku University

Miura, Yohei
Institute for Materials Research, Tohoku University

Takamura, Hitoshi
Graduate School of Engineering, Tohoku University

他



出版情報：MATERIALS TRANSACTIONS. 52 (4), pp.654-657, 2011-04-01. 公益社団法人 日本金属学会
バージョン：

*Materials Transactions*, Vol. 52, No. 4 (2011) pp. 654 to 657
Special Issue on Advanced Materials for Hydrogen Energy Applications


# Enhanced Electrical Conductivities of Complex Hydrides $Li_2(BH_4)(NH_2)$ and $Li_4(BH_4)(NH_2)_3$ by Melting

Yu Zhou[1,*1], Motoaki Matsuo[1,*2], Yohei Miura[1,*3], Hitoshi Takamura[2], Hideki Maekawa[2], Arndt Remhof[3], Andreas Borgschulte[3], Andreas Züttel[3], Toshiya Otomo[4] and Shin-ichi Orimo[1]

[1]*Institute for Materials Research, Tohoku University, Sendai 980-8577, Japan*
[2]*Graduate School of Engineering, Tohoku University, Sendai 980-8579, Japan*
[3]*Empa, Swiss Federal Laboratories for Materials Science and Technology, Division of Hydrogen and Energy, Dübendorf, 8600, Switzerland*
[4]*Institute of Materials Structure Science, High Energy Accelerator Research Organization, Tsukuba 305-0801, Japan*

The electrical conductivities of complex hydrides $Li_2(BH_4)(NH_2)$ and $Li_4(BH_4)(NH_2)_3$ consisting of $(BH_4)^-$ and $(NH_2)^-$ anions are investigated focusing on their low melting temperatures (365 K for $Li_2(BH_4)(NH_2)$ and 490 K for $Li_4(BH_4)(NH_2)_3$). The two hydrides show lithium fast-ion conductivities of about $1 \times 10^{-4}$ S·cm$^{-1}$ at room temperature. After melting, the total ion conductivities of $Li_2(BH_4)(NH_2)$ and $Li_4(BH_4)(NH_2)_3$ reach $6 \times 10^{-2}$ S·cm$^{-1}$ (378 K) and $2 \times 10^{-1}$ S·cm$^{-1}$ (513 K), respectively. The crystal structure and local atomistic structures closely correlated with the lithium ion conduction before and after melting are also discussed. [doi:10.2320/matertrans.MA201003]

(Received September 15, 2010; Accepted February 3, 2011; Published April 1, 2011)

***Keywords:*** *complex hydride, lithium ion conduction, melting*

## 1. Introduction

We have reported solid-state $Li(BH_4)$, a potential candidate for advanced hydrogen storage materials,[1)] exhibits lithium fast-ion conduction (more than $1 \times 10^{-3}$ S·cm$^{-1}$ over 390 K).[2–5)] The development of lithium ion conductors is important because of their potential applications as solid electrolytes for lithium ion batteries. Although a wide variety of lithium fast-ion conductors such as oxides[6,7)] and sulfides[8–11)] have been reported, no lithium fast-ion conductors of hydrides except $Li(BH_4)$ has been found since the report of $Li_2(NH)$ in 1979.[12)] The experimental results on the lithium fast-ion conduction in $Li(BH_4)$ strongly implies that complex hydrides with various combinations of hydrogen-based complex anions such as $(BH_4)^-$, $(NH_2)^-$, $(AlH_4)^-$, $(NH)^{2-}$, $(AlH_6)^{3-}$, and $(NiH_4)^{4-}$ are potential lithium ion conductors.

We have recently reported the lithium fast-ion conductions in $Li_2(BH_4)(NH_2)$ and $Li_4(BH_4)(NH_2)_3$ consisting of $(BH_4)^-$ and $(NH_2)^-$ anions,[13,14)] which have been investigated from the viewpoint of hydrogen storage so far.[15–19)] Further, $Li_2(BH_4)(NH_2)$ and $Li_4(BH_4)(NH_2)_3$ melt at temperatures around 360 K and 460 K,[16)] indicating the possible enhancement of total ion conductivity in these temperature ranges. There has been no report on inorganic lithium fast-ion conductors with such low melting temperatures.

In this study, therefore, we have investigated the electrical conductivities of $Li_2(BH_4)(NH_2)$ and $Li_4(BH_4)(NH_2)_3$ focusing on the melting processes.

## 2. Experimental Procedures

$Li_2(BH_4)(NH_2)$ and $Li_4(BH_4)(NH_2)_3$ were prepared by mechanically milling the mixtures of $Li(BH_4)$ (Aldrich, >95%) and $Li(NH_2)$ (Aldrich, >95%) with molar ratios of 1 : 1 and 1 : 3 for 3.6 ks. The mixtures were then heat treated at 333 K (molar ratio: 1 : 1) and 403 K (1 : 3) for 36 ks under argon to eliminate the defects induced by mechanical milling and increase crystallinity sufficiently. The electrical conductivities were determined in heating and cooling runs by AC complex impedance method using a HIOKI 3532-80 impedance analyzer with molybdenum electrodes from 303 to 378 K for $Li_2(BH_4)(NH_2)$ and from 303 to 513 K for $Li_4(BH_4)(NH_2)_3$. The samples were also examined by powder X-ray diffractometry (XRD, Cu-K$\alpha$ radiation) and Raman spectroscopy (with color-CCD, 532-nm laser). Lattice parameters were determined by using the RIETAN-2000 software package.[20)] Thermal analysis was carried out by differential scanning calorimetry (DSC) under helium atmosphere. Samples were always handled in a glove box filled with purified argon (less than 0.1 ppm oxygen and the dew point below 180 K).

## 3. Results and Discussion

As shown in Fig. 1(a), both $Li_2(BH_4)(NH_2)$ and $Li_4(BH_4)(NH_2)_3$ exhibit fast-ion conductivity of $1 \times 10^{-4}$ S·cm$^{-1}$ at room temperature (*RT*), and the conductivities monotonically increase upon heating. From the results of DSC measurements (Fig. 1(b)) and optical microscopic observations (Fig. 1(c)), the melting temperatures of $Li_2(BH_4)(NH_2)$ and $Li_4(BH_4)(NH_2)_3$ are estimated to be 365 K and 490 K, respectively. The activation energy for conduction, as summarized in Table 1, significantly decrease after melting from 63.7 kJ·mol$^{-1}$ (303–348 K) to 23.2 kJ·mol$^{-1}$ (above 369 K) for $Li_2(BH_4)(NH_2)$. On the other hand, the activation energy slightly increases from 29.9 kJ·mol$^{-1}$ (303–443 K) to 35.7 kJ·mol$^{-1}$ (above 490 K) for $Li_4(BH_4)(NH_2)_3$, which might be attributed to the high viscosity after melting.[21)] The total ion conductivities presumably including the contribu-

*1Graduate Student, Tohoku University
*2Corresponding author, E-mail: mmatsuo@imr.tohoku.ac.jp
*3Present address: NGK INSULATORS, LTD.

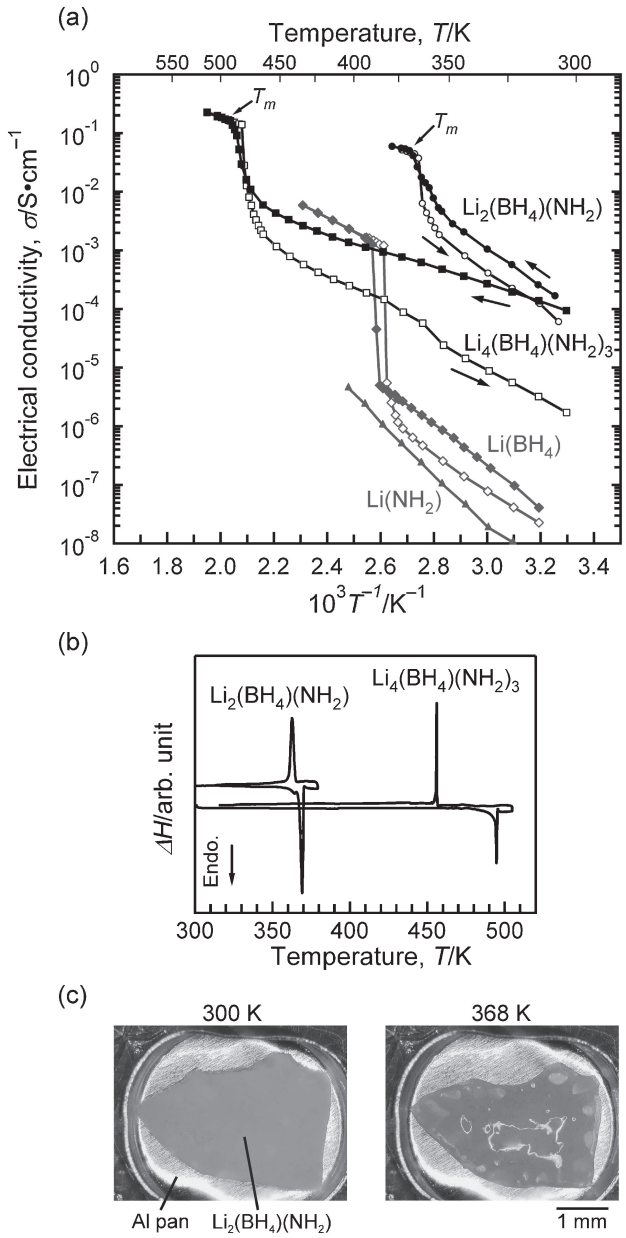


Fig. 1 (a) Electrical conductivities of $Li_2(BH_4)(NH_2)$ (circle) and $Li_4(BH_4)(NH_2)_3$ (square) based on the data in Refs. 13) and 14). The melting temperatures (365 K for $Li_2(BH_4)(NH_2)$ and 490 K for $Li_4(BH_4)(NH_2)_3$) are indicated as $T_m$. For reference, the data of $Li(BH_4)$ and $Li(NH_2)$ are also shown. Close and open symbols denote data obtained in heating and cooling runs, respectively. Differences of conductivities between upon heating and upon cooling are due to phase separations after melting. (b) DSC curves detecting the melting and solidification (endothermic reactions for heating and exothermic ones for cooling, respectively). (c) Optical microscopy images of $Li_2(BH_4)(NH_2)$ before (300 K) and after (368 K) melting.

tions of the $(BH_4)^-$ and $(NH_2)^-$ anions as well as $Li^+$ reach $6 \times 10^{-2}$ S·cm$^{-1}$ (378 K) and $2 \times 10^{-1}$ S·cm$^{-1}$ (513 K) for $Li_2(BH_4)(NH_2)$ and $Li_4(BH_4)(NH_2)_3$ after melting, respectively. It is interesting to note that extrapolated conductivities of $Li_2(BH_4)(NH_2)$ after melting to higher temperatures reach those of $Li_4(BH_4)(NH_2)_3$, suggesting the similarities of the structure and the dynamics after melting.

Here we focus on the local atomistic structures consisting of the $(BH_4)^-$ and $(NH_2)^-$ anions in $Li_2(BH_4)(NH_2)$ and $Li_4(BH_4)(NH_2)_3$ before and after melting. The states of atomic vibrations examined by *in situ* Raman spectroscopy during heating are shown in Fig. 2. The B-H stretching mode (2300 cm$^{-1}$) in $(BH_4)^-$ anions[22] and the N-H stretching modes (3260 and 3320 cm$^{-1}$) in $(NH_2)^-$ anions[23] are clearly detected for both hydrides at *RT*. All these modes are observed even after melting with unaltered Raman shifts. These results provide evidence that the anions actually remain intact within molten $Li_2(BH_4)(NH_2)$ and $Li_4(BH_4)(NH_2)_3$, which has been also reported by first-principles molecular dynamics study.[24] The bandwidth of the B-H stretching mode becomes broader after melting in both the hydrides, which may be due to coupling between the internal stretching mode and the external librational motion by disordering of the $(BH_4)^-$ sublattice.[22] On the other hand, no obvious change of the bandwidth of the N-H stretching modes is observed, indicating that the $(NH_2)^-$ anions may hold a rigid sublattice even after melting.

The crystal structures of $Li_2(BH_4)(NH_2)$ and $Li_4(BH_4)(NH_2)_3$ before melting (as prepared) and after solidification were investigated by XRD, as shown in Fig. 3, and the lattice constants are summarized in Table 2. As prepared samples are well identified to be the single phases of $Li_2(BH_4)(NH_2)$ and $Li_4(BH_4)(NH_2)_3$, respectively; other peaks originated from related compounds such as $Li_2(NH)$ or $Li_3N$ are not observed. Sharp peaks observed for the as prepared samples confirm the sufficient crystal growth by heat treatment (more than 100–200 nm). For $Li_2(BH_4)(NH_2)$, after melting and subsequent solidification, the original peaks disappear and,

Table 1 Activation energies for conduction of $Li_2(BH_4)(NH_2)$ and $Li_4(BH_4)(NH_2)_3$ before and after melting and after solidification.

| Hydride | Activation energy, $E_a$/kJ·mol$^{-1}$ | | |
|---|---|---|---|
| | Before melting | After melting | After solid. |
| $Li_2(BH_4)(NH_2)$ | 63.7 (303–348 K) | 23.2 (above 369 K) | 63.7 (306–354 K) |
| $Li_4(BH_4)(NH_2)_3$ | 29.9 (303–443 K) | 35.7 (above 490 K) | 58.9 (313–382 K) |

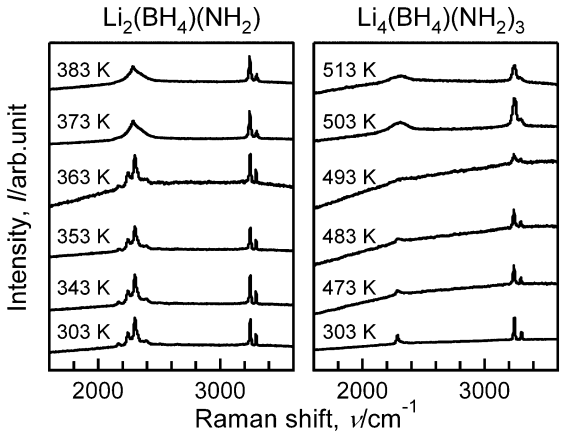


Fig. 2 *In situ* Raman spectra of $Li_2(BH_4)(NH_2)$ and $Li_4(BH_4)(NH_2)_3$ during heating. The beginnings of melting for $Li_2(BH_4)(NH_2)$ at 363 K and for $Li_4(BH_4)(NH_2)_3$ at 493 K made relatively large backgrounds.

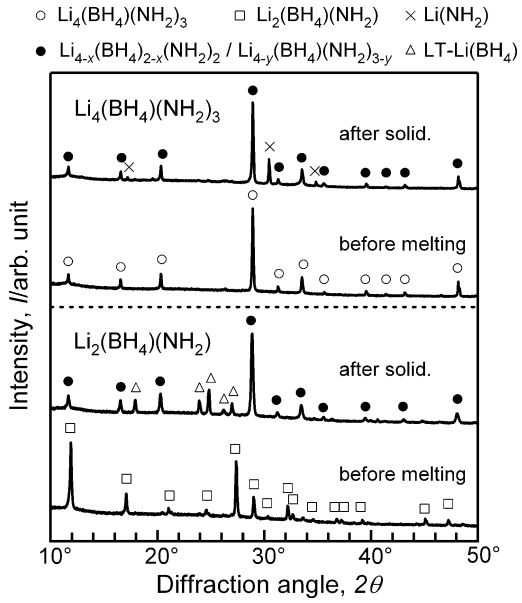


Fig. 3 XRD profiles of $Li_2(BH_4)(NH_2)$ and $Li_4(BH_4)(NH_2)_3$ measured before melting (as prepared) and after solidification.

Table 2 Lattice parameters of $Li_2(BH_4)(NH_2)$ and $Li_4(BH_4)(NH_2)_3$ before melting and after solidification. Calculated standard deviations in parentheses.

| Hydride | Space group | Lattice constant, /nm |
|---|---|---|
| Before melting | | |
| $Li_2(BH_4)(NH_2)$ | trigonal, $R\bar{3}$ | $a = 1.4491(7)$, $c = 0.9242(4)$ |
| After solidification | | |
| $Li_{4-x}(BH_4)_{2-x}(NH_2)_2$ | cubic, $I2_13$ | $a = 1.0711(5)$ |
| $Li(BH_4)$ (LT phase) | orthorhombic, *Pnma* | $a = 0.7176(4)$, $b = 0.4437(4)$, $c = 0.6803(6)$ |
| Before melting | | |
| $Li_4(BH_4)(NH_2)_3$ | cubic, $I2_13$ | $a = 1.0674(2)$ |
| After solidification | | |
| $Li_{4-y}(BH_4)(NH_2)_{3-y}$ | cubic, $I2_13$ | $a = 1.0672(4)$ |
| $Li(NH_2)$ | tetragonal, $I\bar{4}$ | $a = 0.5044(5)$, $c = 1.0279(2)$ |
| $Li_3(BH_4)(NH_2)_2$ | cubic, $I2_13$ | $a = 1.0725(2)$ |

alternatively, those of $Li(BH_4)$ (low temperature phase (LT)) and a body centered cubic phase similar with $Li_4(BH_4)(NH_2)_3$ are observed. Similarly, for $Li_4(BH_4)(NH_2)_3$, the diffraction peaks of $Li(NH_2)$ and a body centered cubic phase are found after melting and solidification.

Judging from the proposed phase diagrams in which nonstoichiometric body centered cubic phases exist between $Li_3(BH_4)(NH_2)_2$, which is a metastable phase, and $Li_4(BH_4)(NH_2)_3$,[16,25] phase separations should occur in both $Li_2(BH_4)(NH_2)$ and $Li_4(BH_4)(NH_2)_3$ after melting and subsequent solidification as follows (Fig. 4):

$$2Li_2(BH_4)(NH_2) \rightarrow Li_{4-x}(BH_4)_{2-x}(NH_2)_2 + xLi(BH_4) \quad (1)$$

$$Li_4(BH_4)(NH_2)_3 \rightarrow Li_{4-y}(BH_4)(NH_2)_{3-y} + yLi(NH_2) \quad (2)$$

The $Li_{4-x}(BH_4)_{2-x}(NH_2)_2$ and $Li_{4-y}(BH_4)(NH_2)_{3-y}$ should have equilibrium compositions corresponding to $Li(BH_4) : Li(NH_2) = 1 : 2.62–1 : 2.83$ or the range of $x$ and $y$ should be $1.24 \leq x \leq 1.29$, $0.17 \leq y \leq 0.38$.[25] The values $x$ and $y$ could be calculated by the linear relation of lattice constants between $Li_3(BH_4)(NH_2)_2$ and $Li_4(BH_4)(NH_2)_3$, based on the Vegard's law. However, the lattice constants of the nonstoichiometric phases are not sensitive to their compositions,[25] as summarized in Table 2. Thus, more reliable method is needed to determine $x$ and $y$ with reasonable precision for this material system.[26]

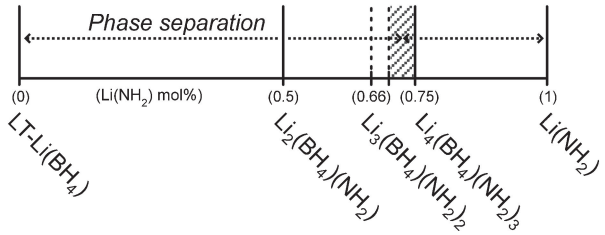


Fig. 4 Phase separations of $Li_2(BH_4)(NH_2)$ and $Li_4(BH_4)(NH_2)_3$. The horizontal axis indicates the molar ratio of $Li(NH_2)$. Hatched area indicates nonstoichiometric compositions such as $Li_{4-x}(BH_4)_{2-x}(NH_2)_2$ and $Li_{4-y}(BH_4)(NH_2)_{3-y}$.

It should be noted that, as shown in Fig. 1 and Table 1, the activation energy for conduction of $Li_2(BH_4)(NH_2)$ upon cooling is rather similar to that upon heating although the conductivities decrease due to the coexistence of the LT phase $Li(BH_4)$. The same tendency is also observed for $Li_4(BH_4)(NH_2)_3$. These results indicate that $Li_{4-x}(BH_4)_{2-x}(NH_2)_2$ and $Li_{4-y}(BH_4)(NH_2)_{3-y}$ formed after solidification might have combined features of $Li_4(BH_4)(NH_2)_3$ and $Li_2(BH_4)(NH_2)$, i.e., the long-range ordering is similar to that of $Li_4(BH_4)(NH_2)_3$,[15–19] and the local structure closely correlated with the migration of $Li^+$ is similar to that of $Li_2(BH_4)(NH_2)$[13] because of the defects of $Li^+$ and $(BH_4)^-$/$(NH_2)^-$. Systematic studies of detailed local atomistic structure of defect-containing $Li_4(BH_4)(NH_2)_3$ as well as ion transport mechanisms of $Li_2(BH_4)(NH_2)$ and $Li_4(BH_4)(NH_2)_3$ after melting by neutron diffraction[27] will be conducted.

## 4. Conclusions

We investigated the electrical conductivities of $Li_2(BH_4)(NH_2)$ and $Li_4(BH_4)(NH_2)_3$ focusing on the melting processes. The two complex hydrides exhibited lithium fast-ion conductivities of about $1 \times 10^{-4}\,S{\cdot}cm^{-1}$ at room temperature. After melting, the total ion conductivities reached $6 \times 10^{-2}\,S{\cdot}cm^{-1}$ (378 K) and $2 \times 10^{-1}\,S{\cdot}cm^{-1}$ (513 K) for $Li_2(BH_4)(NH_2)$ and $Li_4(BH_4)(NH_2)_3$, respectively. Both $(BH_4)^-$ and $(NH_2)^-$ complex anions remain intact within $Li_2(BH_4)(NH_2)$ and $Li_4(BH_4)(NH_2)_3$ even after melting. X-ray diffractometry confirmed that body centered cubic phases, which are isomorphic with $Li_4(BH_4)(NH_2)_3$, formed in $Li(BH_4)$-rich compositions by phase separation of $Li_2(BH_4)(NH_2)$ and $Li_4(BH_4)(NH_2)_3$ after melting and solidification. The solid state body centered cubic phases were found to show ion conductive behavior similar to that of $Li_2(BH_4)(NH_2)$ rather than that of $Li_4(BH_4)(NH_2)_3$.

## Acknowledgements

This work was partially supported by MEXT, Japan (Global COE Program "Materials Integration, Tohoku University" and KAKENHI (21246100 and 22760529) and the Integrated Project of ICC-IMR.

## REFERENCES

1) S. Orimo, Y. Nakamori, J. R. Eliseo, A. Züttel and C. M. Jensen: Chem. Rev. **107** (2007) 4111–4132.
2) M. Matsuo, Y. Nakamori, S. Orimo, H. Maekawa and H. Takamura: Appl. Phys. Lett. **91** (2007) 224103-1–3.
3) M. Matsuo, H. Takamura, H. Maekawa, H.-W. Li and S. Orimo: Appl. Phys. Lett. **94** (2009) 084103-1–3.
4) H. Maekawa, M. Matsuo, H. Takamura, M. Ando, Y. Noda, T. Karahashi and S. Orimo: J. Am. Chem. Soc. **131** (2009) 894–895.
5) H. Oguchi, M. Matsuo, J. S. Hummelshøj, T. Vegge, J. K. Nørskov, T. Sato, Y. Miura, H. Takamura, H. Maekawa and S. Orimo: Appl. Phys. Lett. **94** (2009) 141912-1–3.
6) Y. Inaguma, C. Liquan, M. Itoh, T. Nakamura, T. Uchida, H. Ikuta and M. Wakihara: Solid State Commun. **86** (1993) 689–693.
7) A. Martínez-Juárez, J. M. Rojo, J. E. Iglesias and J. Sanz: Chem. Mater. **7** (1995) 1857–1862.
8) M. Tachez, J. P. Malugani, R. Mercier and G. Robert: Solid State Ionics **14** (1984) 181–185.
9) K. Takada, N. Aotani, K. Iwamoto and S. Kondo: Solid State Ionics **86–88** (1996) 877–882.
10) R. Kanno and M. Murayama: J. Electrochem. Soc. **148** (2001) A742–A746.
11) F. Mizuno, A. Hayashi, K. Tadanaga and M. Tatsumisago: Adv. Mater. **17** (2005) 918–921.
12) B. A. Boukamp and R. A. Huggins: Phys. Lett. A **72** (1979) 464–466.
13) M. Matsuo, A. Remhof, P. Martelli, R. Caputo, M. Ernst, Y. Miura, T. Sato, H. Oguchi, H. Maekawa, H. Takamura, A. Borgschulte, A. Züttel and S. Orimo: J. Am. Chem. Soc. **131** (2009) 16389–16391.
14) M. Matsuo and S. Orimo: Adv. Ener. Mater. in press.
15) T. Noritake, M. Aoki, S. Towata, A. Ninomiya, Y. Nakamori and S. Orimo: Appl. Phys. A **83** (2006) 277–279.
16) G. P. Meisner, M. L. Scullin, M. P. Balogh, F. E. Pinkerton and M. S. Meyer: J. Phys. Chem. B **110** (2006) 4186–4192.
17) P. A. Chater, W. I. F. David, S. R. Johnson, P. P. Edwards and P. A. Anderson: Chem. Commun. (2006) 2439–2441.
18) P. A. Chater, W. I. F. David and P. A. Anderson: Chem. Commun. (2007) 4770–4772.
19) H. Wu, W. Zhou, T. J. Udovic, J. J. Rush and T. Yildirim: Chem. Mater. **20** (2008) 1245–1247.
20) F. Izumi and T. Ikeda: Mater. Sci. Forum **321–324** (2000) 198–203.
21) Electrochemical Aspects of Ionic Liquids, edited by H. Ohno (Wiley Interscience, New York, 2005) p. 62–69.
22) S. Gomes, H. Hagemann and K. Yvon: J. Alloy. Compd. **346** (2004) 206–210.
23) J. P. O. Bohger, R. R. Eßmann and H. Jacobs: J. Mol. Struct. **348** (1995) 325–328.
24) D. E. Farrell, D. Shin and C. Wolverton: Phys. Rev. B **80** (2009) 224201-1–7.
25) J. P. Singer, M. S. Meyer, R. M. Speer, Jr., J. E. Fischer and F. E. Pinkerton: J. Phys. Chem. C **113** (2009) 18927–18934.
26) The validity of formation of stoichiometric $Li_4(BH_4)(NH_2)_3$ after sample preparation is that nonstoichiometric body centered cubic phases are not stable at the heat treatment temperature 403 K.
27) Y. Kawakita, S. Tahara, H. Fujii, S. Kohara and S. Takeda: J. Phys.: Condens. Matter **19** (2007) 335201-1–16.